Juan Du
Mem. ASME
Department of Industrial Engineering and Management,
School of Mechanical Engineering,
Shanghai Jiao Tong University,
Shanghai 200240, China
e-mail: juan.du@sjtu.edu.cn

Changhui Liu[1]
Mem. ASME
School of Mechanical Engineering,
Tongji University,
Shanghai 201804, China
e-mail: liuchanghui@tongji.edu.cn

Jianfeng Liu
Shanghai Waigaoqiao Shipbuilding Co., Ltd.,
Shanghai 200137, China
e-mail: liujianfeng@chinasws.com

Yansong Zhang
School of Mechanical Engineering,
Shanghai Jiao Tong University,
Shanghai 200240, China
e-mail: zhangyansong@sjtu.edu.cn

Jianjun Shi
Fellow ASME
H. Milton Stewart School of Industrial and Systems Engineering,
Georgia Institute of Technology,
Atlanta, GA 30332
e-mail: jianjun.shi@isye.gatech.edu

Optimal Design of Fixture Layout for Compliant Part With Application in Ship Curved Panel Assembly

In a ship assembly process, a large number of compliant parts are involved. The ratio of the part thickness to the length or the width is typically 0.001–0.012. Fixture design is a critical task in the ship assembly process due to its impact on the deformation and dimensional variation of the compliant parts. In current practice, fixtures are typically uniformly distributed under the part to be assembled, which is non-optimal, and large dimensional gaps may occur during assembly. This paper proposed a methodology for the optimal design of the fixture layout in the ship assembly process by systematically integrating direct stiffness method and simulated annealing algorithm, which aims to minimize dimensional gaps along the assembly interface to further improve the quality and efficiency of seam welding. The case study shows that the proposed method significantly reduced the dimensional gaps of the compliant curved panel parts in a ship assembly process.
[DOI: 10.1115/1.4048954]

Keywords: fixture design, ship assembly, direct stiffness method, simulated annealing, compliant part assembly

1 Introduction

The compliant part assembly is common in manufacturing industries such as automobile, aircraft, and ship manufacturing. The design of the fixture layout is a critical task during the assembly process since it defines the locations of fixtures, which can significantly affect the deformation and the dimensional variation of a compliant part, especially when the ratio of the part thickness to the length or the width is very small. Thus, the optimal design of the fixture layout is important to improve the assembly dimensional quality.

In a ship assembly process, a large number of compliant parts are involved. In addition, the compliant panel used for the ship assembly is thin nowadays [1,2], where the ratio of the part thickness to the length or the width is 0.001–0.012 [3]. Thus, the parts are usually deformed under gravity during the ship panel assembly process, which leads to various dimensional gaps along the assembly interface. The dimensional gaps along the edges of two parts to be assembled have a significant contribution to welding deformation [4,5] and also affect the welding quality by introducing internal defects, such as incomplete penetration and fusion, inclusion, undercut, slag, gas pole, and crack [6]. In the current practice of the ship assembly process, dimensional gaps should be corrected to meet tolerance requirements by trimming and correction before welding the compliant panels. However, it is very time-consuming and seriously reduces the production efficiency. Therefore, it is of great significance if we can reduce the dimensional gaps of ship curved panels during the assembly process by optimizing the fixture layout.

In general, the current methodologies for the optimal design of the fixture layout can be classified into two categories according to the mechanical property of the part. The first category deals with the fixture design for the rigid parts. For example, De Meter [7] proposed a min-max load model for optimizing the design of the fixture layout in the machining process. Cai et al. [8] proposed a variational method for the robust fixture design of the 3D workpiece. Kim and Ding [9] proposed a revised exchange algorithm for the optimal design of fixture layouts in multi-station assembly processes based on a two-dimensional, rigid panel assembly model. Kim and Ding [10] further proposed a data-mining–aided optimal design method for the fixture layout. Based on these works, Phoomboplab and Ceglarek [11] proposed a methodology based on genetic algorithm and Hammersley sequence sampling for the optimal design of fixture layouts in three-dimensional multi-station assembly systems. To consider critical product dimensions, Söderberg and Carlson [12] proposed a scheme for sensitivity analysis, and Lööf et al. [13] optimized the fixture layout to maximize robustness. Söderberg et al. [14] discussed the scheme optimization from a physical dependency perspective. All these methods work well for the rigid parts, but cannot be applied in the fixture design of the compliant part assembly.

The other category is the optimal design of the fixture layout for the compliant parts. Early methods for the optimal design of the fixture layout are mainly dependent on a quantity of finite element analysis (FEA). For example, Rearick et al. [15] used cost function analysis to determine the optimal fixture layout for deformable sheet metal parts. Cai and Hu [16] proposed an

[1]Corresponding author.

Manuscript received June 21, 2020; final manuscript received October 19, 2020; published online December 17, 2020. Assoc. Editor: Ran Jin.

optimal fixture configuration design by considering deformation and assembly spring back of sheet metal parts. Based on the "3-2-1" principle for the rigid parts, Cai et al. [17] further proposed an "*N*-2-1" principle ($N \geq 3$) for the deformable sheet metal parts. The effectiveness of fixture design for compliant parts strongly depends on the layout of the *N* locating points, and Cai et al. [17] used FEA and nonlinear programming methods to find the best *N* locating points. Based on this principle, Das et al. [18] proposed a fixture design optimization method by considering the production batch of non-ideal parts, and Franciosa et al. [19] introduced the measure of fixture capability to determine the optimal layout of fixtures. Kulankara et al. [20] proposed a genetic-algorithm based procedure for optimizing fixture layout. Menassa and DeVries [21] proposed a method to assist the selections of fixture locations by using optimization techniques, and the method is demonstrated on the prismatic parts. Dahlström and Camelio [22] proposed a fixture design methodology for the sheet metal assembly using FEA and design of computer experiments. Camelio et al. [23] proposed a fixture design methodology to minimize the assembly variation by combination of FEA and nonlinear programming methods. Liao et al. [24] used FEA for fixture layout optimization with consideration of workpiece–fixture contact interaction. Dou et al. [25] proposed a fixture layout optimization method by integrating ANSYS APDL of FEA and particle swarm optimization algorithm for the reduction of dimensional errors of the workpiece during the machining process. Cai [26] further proposed a fixture optimization method for the sheet panel assembly by considering the welding gun variations.

Recently, to improve the optimization efficiency of fixture layout design, a series of fixture layout optimization methods for the auto-body parts are proposed. For example, Xing et al. [27] proposed to use a non-domination sorting social radiation algorithm for fixture layout optimization of auto parts. An engineering rule is developed to filter out the infeasible candidates of fixture locations to improve the optimization efficiency. A multi-station fixture layout optimization method is further proposed by Xing et al. [28] for sheet metal parts by using the analytic hierarchy process and particle swarm algorithm. To fully automate the fixture layout optimization procedures, Xing [29] combined 3DCs for dimensional analyses and global optimization algorithms. Notably, all of these methods need FEA software for the calculation of part deformation or dimensional analysis, and the methods mainly targeted on auto-body applications. To avoid the intensive FEA calculation during the optimal fixture design process, Yang et al. [30] proposed a surrogate model to approximate the FEA calculation based on Kriging for the sheet metal parts. Lu and Zhao [31] proposed a neural network model for surrogate modeling to replace the FEA calculation. However, the surrogate model cannot be always accurately established, which is dependent on the structure and part property. In addition, surrogate modeling also needs the training dataset and testing dataset from the design of experiments (DOEs) by FEA.

Similar to other deformable sheet part assembly process, the "*N*-2-1" locating principle [17] is also adopted in the ship curved panel assembly. Different from spot welding used in the auto-body assembly, seam welding is needed in the ship curved panel assembly, thereby indicating the dimensional gaps along the assembly interface between two compliant parts will significantly affect the welding quality. Thus, the key objective in the optimal design of the fixture layout for the ship curved panel assembly is to minimize dimensional gaps along the interface between the two compliant parts to be assembled. However, the existing fixture design methods try to minimize the overall part deformation, without considering the dimensional gaps along the assembly interface [17,21]. Due to the small ratio of the part thickness to the length or the width and large dimension of the compliant parts, significant part deformations will be induced by gravity and further result in large dimensional gaps along the assembly interface in the ship curved panel assembly process. Therefore, more locators on the primary datum are needed for the ship curved panel assembly, which means that the "*N*" is very large in the "*N*-2-1" principle. On the other hand, a large number of possible candidate locations exist to place locators for the ship curved panels because of its large physical dimensions. As a result, a more effective method should be proposed for the optimal design of fixtures in the ship assembly.

In this paper, we proposed an optimal design of fixture layout methodology (called DSMSO) by systematically integrating direct stiffness method (DSM) and stochastic optimization (SO) technique for the compliant part assembly with a demonstration in ship manufacturing industry. Our methodology is under the "*N*-2-1" principle of Cai et al. [17] and mainly aims to find the optimal *N* locating points from all the candidate points, which are the meshed nodes on the compliant parts to be assembled. The DSMSO method considers the dimensional gaps along the assembly interface induced by gravity between two compliant parts to be assembled, and aims to minimize such dimensional gaps by optimizing the fixture layouts. Specifically, we first derive the DSM for the fixture design setting and formulate the fixture design problem as a binary integer programming problem. Then, the simulated annealing algorithm is adopted to solve the optimization problem. Notably, we can get the exact deformation given the fixture condition via DSM without intensive implementations of FEA software. In addition, compared with the surrogate modeling, our method can get the accurate solution instead of an approximation, and there is no need for design of experiments and corresponding collections of training and testing datasets.

Notably, the current literature on the optimal design of the fixture layout mainly focuses on minimizing the deformation of a single part without considering the dimensional gaps along the edge of two parts to be assembled. However, how to minimize those gaps is an important problem in seam welding in the ship curved panel assembly process. Our DSMSO method will minimize dimensional gaps along the edges of two parts to be assembled and also consider the overall surface profile tolerance of each part for the optimal design of the fixture layout. Thus, the DSMSO method will provide smaller dimensional gaps and further improve the quality and efficiency of seam welding.

The remainder of this paper is organized as follows. Section 2 develops the proposed methodology for the optimal design of the fixture layout. In Sec. 3, a case study in the curved ship panel assembly process is used to demonstrate the proposed method. Finally, the conclusions are summarized in Sec. 4.

2 DSMSO Methodology for Optimal Design of Fixture Layout

An overview of the proposed DSMSO method is shown in Fig. 1. According to the FEA model, the global stiffness matrix and global load vector can be exported. Then, a modified direct stiffness method is proposed for the fixture design problem to facilitate the calculation of the modified stiffness matrix and modified load vector. A binary integer programming formulation is further proposed for optimizing the fixture layouts. Finally, a simulated annealing algorithm is adopted for the solution of the binary integer programming problem.

Since the proposed method is established based on DSM, we will first briefly introduce DSM in Sec. 2.1. Afterwards, a binary integer programming formulation of fixture design is developed in Sec. 2.2. To solve the optimization problem, a simulated annealing algorithm will be discussed in Sec. 2.3.

2.1 Introduction to the Direct Stiffness Method. The DSM is the realization of FEA, and all major commercial FEA software are based on DSM [32]. In the DSM, the global stiffness matrix and global force vector are assembled according to the element stiffness matrix and the consistent nodal force vector. The assembly

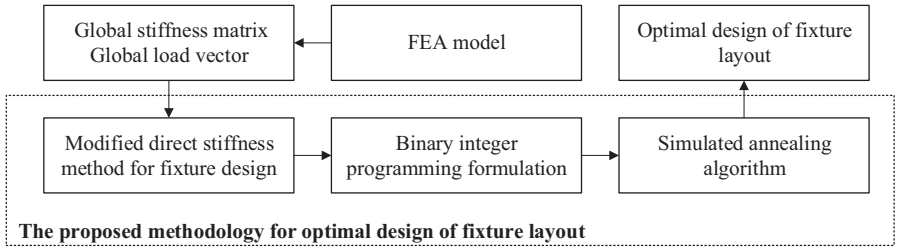

Fig. 1 Flowchart of the proposed DSMSO method

result is the global stiffness equation

$$\mathbf{Ku} = \mathbf{f} \tag{1}$$

where $\mathbf{K} \in \mathrm{R}^{n\times n}$, $\mathbf{u} \in \mathrm{R}^n$, and $\mathbf{f} \in \mathrm{R}^n$ are the global stiffness matrix, nodal displacement vector, and nodal force vector, respectively. n is the number of nodal displacements of the part. The full representation of the global stiffness equation (1) is

$$\begin{bmatrix} k_{11} & k_{12} & k_{13} & \dots & k_{1n} \\ k_{21} & k_{22} & k_{23} & \dots & k_{2n} \\ k_{31} & k_{32} & k_{33} & \dots & k_{3n} \\ \vdots & \vdots & \vdots & \ddots & \vdots \\ k_{n1} & k_{n2} & k_{n3} & \dots & k_{nn} \end{bmatrix} \begin{Bmatrix} u_1 \\ u_2 \\ u_3 \\ \vdots \\ u_n \end{Bmatrix} = \begin{Bmatrix} f_1 \\ f_2 \\ f_3 \\ \vdots \\ f_n \end{Bmatrix} \tag{2}$$

where k_{ij} is the element of the ith row and the jth column of the global stiffness matrix $\mathbf{K}$, and u_i and f_i are the ith element of nodal displacement $\mathbf{u}$ and nodal force $\mathbf{f}$, respectively. Equation (2) cannot be directly solved due to the singular condition of $\mathbf{K}$ matrix. Thus, physical support should be imposed to eliminate the rigid body motions, which is called displacement boundary conditions. In fact, fixtures are one kind of physical supports, so placement of fixtures is equivalent to adding displacement boundary conditions.

In the literature, the conventional modifications of Eq. (2) to impose displacement boundary conditions are illustrated in Ref. [32]. Suppose the tth element of nodal displacement $\mathbf{u}$, i.e., u_t, is known and $u_t = \bar{u}_t$. The conventional way to impose displacement boundary conditions is to set $k_{tt} = 1, f_t = \bar{u}_t$, and $k_{it} = k_{ti} = 0$ of the global stiffness equation for $i = 1, 2, \dots, n$ and $i \neq t$. For example, if $t = 2$, i.e., $u_2 = \bar{u}_2$ is known, then the modified equation from the global stiffness equation is

$$\begin{bmatrix} k_{11} & 0 & k_{13} & \dots & k_{1n} \\ 0 & 1 & 0 & \dots & 0 \\ k_{31} & 0 & k_{33} & \dots & k_{3n} \\ \vdots & \vdots & \vdots & \ddots & \vdots \\ k_{n1} & 0 & k_{n3} & \dots & k_{nn} \end{bmatrix} \begin{Bmatrix} u_1 \\ u_2 \\ u_3 \\ \vdots \\ u_n \end{Bmatrix} = \begin{Bmatrix} \overline{f_1} \\ \bar{u}_2 \\ \overline{f_3} \\ \vdots \\ \overline{f_n} \end{Bmatrix} \tag{3}$$

Such modified stiffness equation can be denoted as $\bar{\mathbf{K}}u = \bar{\mathbf{f}}$, and $\bar{\mathbf{K}} \in \mathrm{R}^{n\times n}$ and $\bar{\mathbf{f}} \in \mathrm{R}^n$ are modified global stiffness matrix and the nodal force vector, respectively. However, the modified equation (3) is ill-conditioned, and the associated solution is sensitive to small perturbations in the modified global stiffness matrix $\bar{\mathbf{K}}$ and the nodal force vector $\bar{\mathbf{f}}$. To overcome this limitation, Wu et al. [33] proposed an improved procedure for modifications of Eq. (2) given the displacement boundary conditions. Similarly, suppose u_t is known and $u_t = \bar{u}_t$. Wu et al. [33] proposed to set $f_t = k_{tt}\bar{u}_t$, $\bar{f}_i = f_i - k_{it}\bar{u}_t$, and $k_{it} = k_{ti} = 0$ of the original equation (2) for $i = 1, 2, \dots, n$ and $i \neq t$. For example, if $t = 2$, i.e., $u_2 = \bar{u}_2$ is known, then the modified equation from the global stiffness equation is

$$\begin{bmatrix} k_{11} & 0 & k_{13} & \dots & k_{1n} \\ 0 & k_{22} & 0 & \dots & 0 \\ k_{31} & 0 & k_{33} & \dots & k_{3n} \\ \vdots & \vdots & \vdots & \ddots & \vdots \\ k_{n1} & 0 & k_{n3} & \dots & k_{nn} \end{bmatrix} \begin{Bmatrix} u_1 \\ u_2 \\ u_3 \\ \vdots \\ u_n \end{Bmatrix} = \begin{Bmatrix} \overline{f_1} \\ k_{22}\bar{u}_2 \\ \overline{f_3} \\ \vdots \\ \overline{f_n} \end{Bmatrix} \tag{4}$$

where $\bar{f}_i = f_i - k_{i2}\bar{u}_2$, $i = 1, 3, 4, \dots, n$. Given the modified equation (4), the unknown nodal displacement can be solved. In this paper, we developed the formulation of fixture design problem based on the modifications of Wu et al. [33], which will be illustrated in Sec. 2.2.

2.2 Problem Definition and Formulation. Due to the compliant property of a large ship curved panel, the deformation induced by gravity is significant. In this paper, we mainly consider the optimal design of the fixture layout for the ideal part to reduce the dimensional gap induced by gravity. Given the structure of a compliant part, gravity, meshing strategy, and the element type, the global stiffness matrix $\mathbf{K}$, global nodal force vector $\mathbf{f}$, and the number of nodes are known from the FEA. It is reasonable to assume that the mechanical behavior of the compliant part is linear elastic by imposing the locators, which indicates that the global stiffness matrix $\mathbf{K}$ and the global nodal force vector $\mathbf{f}$ are constant during the fixture design. The size, shape, and material properties of the parts will simultaneously determine the global stiffness matrix $\mathbf{K}$. However, the assumption of linear elastic deformation is the only assumption that the following modified stiffness method works for fixture design problem. By imposing locators on the compliant part, the corresponding nodal displacements will be constrained.

Proposition 1. *For the fixture design setting, suppose $u_t = 0$. To impose such displacement boundary conditions, we only need to set $f_t = 0$, and $k_{it} = 0$ for $i = 1, 2, \dots, n$ and $i \neq t$. For example, if $t = 2$, i.e., $u_2 = 0$, the modified equations are*

$$\begin{bmatrix} k_{11} & k_{12} & k_{13} & \dots & k_{1n} \\ 0 & k_{22} & 0 & \dots & 0 \\ k_{31} & k_{32} & k_{33} & \dots & k_{3n} \\ \vdots & \vdots & \vdots & \ddots & \vdots \\ k_{n1} & k_{n2} & k_{n3} & \dots & k_{nn} \end{bmatrix} \begin{Bmatrix} u_1 \\ u_2 \\ u_3 \\ \vdots \\ u_n \end{Bmatrix} = \begin{Bmatrix} f_1 \\ 0 \\ f_3 \\ \vdots \\ f_n \end{Bmatrix} \tag{5}$$

It is simple to prove that the modified equation (5) can provide the same solution of nodal displacements as Eq. (4) given $u_2 = 0$. Similarly, it can be proved that the revised settings of f_t and k_{it} will also give the same solution as the modified procedure of Wu et al. [33] given the fixture setting $u_t = 0$.

In this paper, we consider the optimal fixture layout for the assembly of two compliant parts. Let n_p denote the number of nodal displacements of the compliant part p, then the number of nodes of the part p is $m_p = n_p/M_p$, where M_p is the degree-of-freedom of the element in part p, $p = 1, 2$. Since surfaces of curved compliant panels may be complex, the candidate locating

points are hardly expressed by equations. Thus, we follow Xing's work [29] and use meshed nodes as locating points that can deal with any sheet metal part. In other words, we suppose that the locators are located at N number of nodes among these m number of total nodes, where $m = m_1 + m_2$ is the total number of meshed nodes of both parts. N is a predefined constant number. Let $x_i \in \{0, 1\}$ be a binary variable, where $x_i = 0$ indicates a locator is placed at node i. Then, the fixture design problem can be formulated as

$$\min_{\boldsymbol{x} \in X} H(\boldsymbol{x})$$

$$\text{s.t. } \bar{\mathbf{K}}_1(\boldsymbol{x})\mathbf{u} = \bar{\mathbf{f}}_1(\boldsymbol{x})$$

$$\bar{\mathbf{K}}_2(\boldsymbol{x})\mathbf{v} = \bar{\mathbf{f}}_2(\boldsymbol{x}) \tag{6}$$

where $\boldsymbol{X} = \{(x_1, x_2, x_3, \ldots, x_m), x_1, x_2, x_3, \ldots, x_m$ is a permutation of $0, \ldots, 0, 1, \ldots, 1\}$ and there are N number of zeros in set $\boldsymbol{X}$, i.e., $\sum_{i=1}^{m} x_i = m - N$. Since the modified equations are dependent on the fixture layouts, we use $\bar{\mathbf{K}}_1(\boldsymbol{x})\mathbf{u} = \bar{\mathbf{f}}_1(\boldsymbol{x})$ and $\bar{\mathbf{K}}_2(\boldsymbol{x})\mathbf{v} = \bar{\mathbf{f}}_2(\boldsymbol{x})$ to denote the modified equations for part I and part II, respectively. $\mathbf{u} \in \mathrm{R}^{n_1}$ and $\mathbf{v} \in \mathrm{R}^{n_2}$ are the displacements of part I and part II. Given $x_i = 0$, the corresponding nodal displacements will be constrained to 0, and $\bar{\mathbf{K}}_p(\boldsymbol{x})$ and $\bar{\mathbf{f}}_p(\boldsymbol{x})$, $p = 1, 2$, will be obtained from Proposition 1. $H(\boldsymbol{x})$ is the objective function for the optimal design of the fixture layout, which can be determined from the engineering requirements. In the ship curved panel assembly process, practitioners hope that the mean of dimensional gaps along the interface under gravity is minimized and the surface profile tolerance of the parts to be assembled meets the required precision ε, where the surface profile tolerance can be characterized by the displacement at each node of the parts. Thus, problem (6) can be further written as

$$\min_{\boldsymbol{x} \in X} H(x) = \sum_{i=1}^{m_0} \psi_i(\boldsymbol{x})/m_0$$

$$\text{s.t. } \bar{\mathbf{K}}_1(\boldsymbol{x})\mathbf{u} = \bar{\mathbf{f}}_1(\boldsymbol{x})$$

$$\bar{\mathbf{K}}_2(\boldsymbol{x})\mathbf{v} = \bar{\mathbf{f}}_2(\boldsymbol{x})$$

$$\sqrt{u_{ix}^2(\boldsymbol{x}) + u_{iy}^2(\boldsymbol{x}) + u_{iz}^2(\boldsymbol{x})} \le \varepsilon, \quad i = 1, 2, \ldots, m_1,$$

$$\sqrt{v_{ix}^2(\boldsymbol{x}) + v_{iy}^2(\boldsymbol{x}) + v_{iz}^2(\boldsymbol{x})} \le \varepsilon, \quad i = 1, 2, \ldots, m_2, \tag{7}$$

where $\boldsymbol{u}(\boldsymbol{x}) = \mathbf{u}$, $\boldsymbol{v}(\boldsymbol{x}) = \mathbf{v}$ given $\bar{\mathbf{K}}_1(\boldsymbol{x})$, $\bar{\mathbf{K}}_2(\boldsymbol{x})$, $\bar{\mathbf{f}}_1(\boldsymbol{x})$, and $\bar{\mathbf{f}}_2(\boldsymbol{x})$. $u_{ix}(\boldsymbol{x})$, $u_{iy}(\boldsymbol{x})$, $u_{iz}(\boldsymbol{x})$, $v_{ix}(\boldsymbol{x})$, $v_{iy}(\boldsymbol{x})$, and $v_{iz}(\boldsymbol{x})$ are linear displacements of the ith node in the x-, y- and z-directions of part I and part II, which are the elements of $\boldsymbol{u}(\boldsymbol{x})$ and $\boldsymbol{v}(\boldsymbol{x})$. $\psi_i(\boldsymbol{x}) = \sqrt{(u_{ix}(\boldsymbol{x}) - v_{ix}(\boldsymbol{x}))^2 + (u_{iy}(\boldsymbol{x}) - v_{iy}(\boldsymbol{x}))^2 + (u_{iz}(\boldsymbol{x}) - v_{iz}(\boldsymbol{x}))^2}$ is the dimensional gap at node i along the interface between the compliant parts to be assembled under gravity and fixture layout $\boldsymbol{x}$. m_0 is the number of nodes along the assembly interface between two parts. Figure 2 shows the nodes along the assembly interface between two parts, and m_0 is the total number of these nodes.

Notably, the whole framework also works when the assembly constraints exist. Let $\boldsymbol{X}_{in}^1$ and $\boldsymbol{X}_{in}^2$ be the infeasible set of nodes that cannot place locators due to the assembly constraints for part I and part II, and card $(\boldsymbol{X}_{in}^1) = c_1$, card $(\boldsymbol{X}_{in}^2) = c_2$. Let $c = c_1 + c_2$, then the cardinality of the feasible set of nodes $\boldsymbol{X}_f$ for the assembly parts is $m - c$, i.e., card $(\boldsymbol{X}_f) = m - c$. Problem (7) can be written as

$$\min_{\boldsymbol{x} \in X_f} H(x) = \sum_{i=1}^{m_0} \psi_i(\boldsymbol{x})/m_0$$

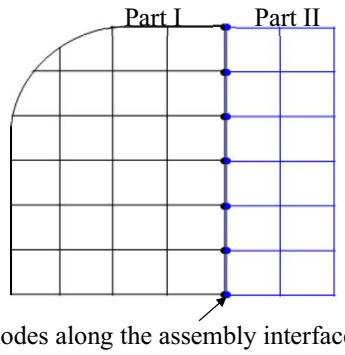

Fig. 2 Illustrations of the nodes along the assembly interface between two parts

$$\text{s.t. } \bar{\mathbf{K}}_1(\boldsymbol{x})\mathbf{u} = \bar{\mathbf{f}}_1(\boldsymbol{x})$$

$$\bar{\mathbf{K}}_2(\boldsymbol{x})\mathbf{v} = \bar{\mathbf{f}}_2(\boldsymbol{x})$$

$$\sqrt{u_{ix}^2(\boldsymbol{x}) + u_{iy}^2(\boldsymbol{x}) + u_{iz}^2(\boldsymbol{x})} \le \varepsilon, \quad i = 1, 2, \ldots, m_1,$$

$$\sqrt{v_{ix}^2(\boldsymbol{x}) + v_{iy}^2(\boldsymbol{x}) + v_{iz}^2(\boldsymbol{x})} \le \varepsilon, \quad i = 1, 2, \ldots, m_2, \tag{8}$$

where $\boldsymbol{X}_f = \{(x_1, x_2, x_3, \ldots, x_{m-c}), x_1, x_2, x_3, \ldots, x_{m-c}$ is a permutation of $0, \ldots, 0, 1, \ldots, 1\}$, and there are N number of zeros in set $\boldsymbol{X}_f$, i.e., $\sum_{i=1}^{m-c} x_i = m - c - N$.

2.3 Algorithm. As the binary integers and complex constraints exist in Eqs. (7) and (8), these two optimization problems are non-convex. In addition, the search space of solution is also large, thereby indicating traditional integer programming methods, such as branch-and bound, divide and conquer, are challenging to be applied [34]. Metaheuristic optimization algorithms are higher-level procedure or frameworks that aim to provide a sufficiently good solution to an optimization problem by efficiently and effectively exploring the search space [35]. Simulated annealing algorithm is one of the metaheuristic optimization methods to handle this kind of non-convex global optimization problem from stochastics with theoretical guarantee [36]. Although it is not guaranteed that the global optimum can be found in practice, the theory of simulated annealing guides us toward better solution via parameter settings. In addition, simulated annealing has an explicit strategy to escape from local optimum by accepting solutions that are worse than current solution with a decreasing probability as iterations increase. Thus, we apply simulated annealing algorithm for solving the optimization problems (7) or (8). Here, we use problem (7) to illustrate the problem-solving procedures.

In the literature, penalty functions have often been used for constrained optimization [37]. The penalty function methods temporarily relax the hardest constraints and use a modified objective function instead to avoid the solution far from the feasible region. The penalty function usually can be represented as $\delta(d(\boldsymbol{x}, \boldsymbol{B}))$, where $d(\boldsymbol{x}, \boldsymbol{B})$ is a metric function describing the decision variables from the hardest constraint $\mathbf{B}$. $\delta(0) = 0$ is satisfied for a penalty function, which indicates no penalty exists if $\boldsymbol{x}$ satisfies constraint $\mathbf{B}$.

Given problem (7), to effectively handle the constraints $\sqrt{u_{ix}^2(\boldsymbol{x}) + u_{iy}^2(\boldsymbol{x}) + u_{iz}^2(\boldsymbol{x})} \le \varepsilon$, $i = 1, 2, \ldots, m_1$, and $\sqrt{v_{ix}^2(\boldsymbol{x}) + v_{iy}^2(\boldsymbol{x}) + v_{iz}^2(\boldsymbol{x})} \le \varepsilon, i = 1, 2, \ldots, m_2$, we first define an indicator function as the penalty function as follows:

$$\delta(\boldsymbol{x}) = \begin{cases} \delta & \boldsymbol{x} \notin C_1 \quad \text{or} \quad \boldsymbol{x} \notin C_2 \\ 0 & \boldsymbol{x} \in C_1 \text{ and } \boldsymbol{x} \in C_2 \end{cases}$$

$$C_1 = \left\{ \boldsymbol{x} \in \boldsymbol{X} : \sqrt{u_{ix}^2(\boldsymbol{x}) + u_{iy}^2(\boldsymbol{x}) + u_{iz}^2(\boldsymbol{x})} \le \varepsilon, \quad i = 1, 2, \ldots, \ m_1 \right\}$$

$$C_2 = \left\{ \boldsymbol{x} \in \boldsymbol{X} : \sqrt{v_{ix}^2(\boldsymbol{x}) + v_{iy}^2(\boldsymbol{x}) + v_{iz}^2(\boldsymbol{x})} \le \varepsilon, \quad i = 1, 2, \ldots, m_2 \right\} \tag{9}$$

where δ is a very large constant. Then, problem (7) can be reformulated as

$$\min_{\boldsymbol{x} \in \boldsymbol{X}} f(\boldsymbol{x}) = \sum_{i=1}^{m_0} \psi_i(\boldsymbol{x}) / m_0 + \ \delta(\boldsymbol{x})$$

$$\text{s.t. } \bar{\mathbf{K}}_1(\boldsymbol{x})\mathbf{u} = \bar{\mathbf{f}}_1(\boldsymbol{x})$$

$$\bar{\mathbf{K}}_2(\boldsymbol{x})\mathbf{v} = \bar{\mathbf{f}}_2(\boldsymbol{x}) \tag{10}$$

To apply the simulated annealing algorithm for problem (10), we first define

$$\Pi^{\beta}(\boldsymbol{x}) = \frac{1}{Z_{\beta}} e^{-\beta f(\boldsymbol{x})}, \quad Z_{\beta} = \sum_{\boldsymbol{x} \in \boldsymbol{X}} \exp(-\beta f(\boldsymbol{x})),$$
$$M_0 = \left\{ \boldsymbol{x}_0 : f(\boldsymbol{x}_0) = \min_{\boldsymbol{x} \in \boldsymbol{X}} f(\boldsymbol{x}) \right\} \tag{11}$$

where $\beta > 0$ is a tuning parameter, and $\Pi^{\beta}(\boldsymbol{x})$ is a probability distribution on $\boldsymbol{X}$. It can be proved that $\Pi^{\beta}(\boldsymbol{x})$ monotonically increases as a function of β for any $\boldsymbol{x} \in M_0$, and monotonically decreases as a function of β for any $\boldsymbol{x} \notin M_0$ if β is sufficiently large [36]. The property of $\Pi^{\beta}(\boldsymbol{x})$ inspires us that we can generate a sequence of random numbers with distribution $\Pi^{\beta}(\boldsymbol{x})$, and it will finally find one of the minimizers as β is infinity. Such construction of $\Pi^{\beta}(\boldsymbol{x})$ enables the global optimization of problem (10), and random number generation can be achieved by Metropolis algorithm [38]. Algorithm 1 shows the simulated annealing algorithm for problem (10).

Algorithm 1 The simulated annealing algorithm for optimal design of fixture layout.

1. **Input**: $\mathbf{K}$, $\mathbf{f}$, L, T, α
2. **Initialize** $\boldsymbol{x}^0 \in \boldsymbol{X}$, β^0
3. **Compute** $f(\boldsymbol{x}^0)$ given $\bar{\mathbf{K}}_1(\boldsymbol{x}^0)$, $\bar{\mathbf{K}}_2(\boldsymbol{x}^0)$, $\bar{\mathbf{f}}_1(\boldsymbol{x}^0)$ and $\bar{\mathbf{f}}_2(\boldsymbol{x}^0)$ from the Proposition 1
4. **Repeat**
5. **For** $i = 0, 1, \ldots, L$
6. Generate a new permutation $\boldsymbol{y} \in \boldsymbol{N}(\boldsymbol{x}^i)$
7. Compute $f(\boldsymbol{y})$ given $\bar{\mathbf{K}}_1(\boldsymbol{y})$, $\bar{\mathbf{K}}_2(\boldsymbol{y})$, $\bar{\mathbf{f}}_1(\boldsymbol{y})$ and $\bar{\mathbf{f}}_2(\boldsymbol{y})$ from the Proposition 1
8. Compute $\Delta f = f(\boldsymbol{y}) - f(\boldsymbol{x}^i)$,
9. Generate a random number $a \sim U[0, 1]$
10. If $\Delta f < 0$ or $a < \mathrm{e}^{-\beta \Delta f}$,
11. $\boldsymbol{x}^{i+1} = \boldsymbol{y}$,
12. Otherwise, $\boldsymbol{x}^{i+1} = \boldsymbol{x}^i$, $f(\boldsymbol{x}^{i+1}) = f(\boldsymbol{x}^i)$
13. **End**
14. $\beta^{j+1} = \alpha\beta^j$, $x^0 = \boldsymbol{x}^{i+1}$, $f(\boldsymbol{x}^0) = f(\boldsymbol{x}^{i+1})$
15. **Until** $\beta^{j+1} \ge T$

In Algorithm 1, $\mathbf{K}$ and $\mathbf{f}$ are the global stiffness matrix and nodal force vector. L is the number of generations in Metropolis algorithm. T is a large number to end the simulated annealing in practice. The neighborhood of a binary state system $\boldsymbol{x} \in \boldsymbol{X}$ is defined as the set $N(\boldsymbol{x})$ with hamming distance equal to 2 from $\boldsymbol{x}$ in our problem. Notably, we use $\beta^{j+1} = \alpha\beta^j$ $(\alpha > 1)$ as the strategy in increasing β, which is widely used in the simulated annealing algorithm [39]. Theoretically, the simulated annealing algorithm can converge to the global optimum of the optimization problem (10) under a sufficient slow increasing rate of β. More details about Metropolis algorithm and simulated annealing can be referred to Ref. [36]. Notably, the algorithm is also valid for the optimization problem (8) given $\boldsymbol{x}^0 \in \boldsymbol{X}_f$, and the neighborhood set $N(\boldsymbol{x})$ is defined with hamming distance equal to 2 from $\boldsymbol{x}$ on feasible set $\boldsymbol{X}_f$.

3 Case Study

In this section, a case study in the ship curved panel assembly process is conducted to illustrate the proposed method for the optimal design of the fixture locator layout. Notably, FEA simulation can exactly simulate real case with high accuracy in terms of linear elastic deformation calculation [40]. The FEA model of the compliant part is elaborated in Sec. 3.1, which is established based on the real dimension and material properties of ship plates. Then, the results of the proposed method are shown in Sec. 3.2. Section 3.3 validates our results by FEA. Finally, discussions are provided in Sec. 3.4.

3.1 Problem Description. In a ship assembly process, a ship curved panel is easy to be deformed under the gravity because of the small ratio of the part thickness to the length or the width. In order to reduce the deformation caused by the gravity, a large number of locators on the primary datum are placed on the ground (x–y plane), where the heights in z-direction can be adjusted according to the surface of the parts, as shown in Fig. 3(*a*). Figure 3(*b*) shows the fixture layout in a ship curved panel assembly process. Due to the simplicity of uniform layout and easier to be adjusted for different types of compliant parts in a ship assembly process, current practice adopts the uniform layout of fixtures to support the part.

In this case study, we take the assembly of two ship parts as an example. Notably, these two ship parts are at the bow where the assembly quality is very critical. Figure 4(*a*) shows their geometries. The lengths of four sides for part I are 5600 mm, 4600 mm, 5500 mm, and 3200 mm, respectively, where the large curved panel is with various radius of curvature. Part II is an approximate rectangle with 5500 mm of length and 600 mm of width. Both of these two parts are 6 mm thick. The density, Young's modulus, and Poisson's ratio of the curved panels are 7.85×10^{-3} g/mm^3, 210,000 N/mm^2 and 0.3, respectively. In order to explore the optimal design of the fixture layout, we establish an FEA model using ABAQUS as shown in Fig. 4(*b*). Specifically, part I is meshed with 2198 number of S4R elements and 60 number of S3 elements in the FEA model, thereby indicating the total number of nodes is 2346. Part II is meshed with 330 number of S4R elements, and the total number of nodes is 392. The gravity is uniformly distributed on the parts, where the direction of gravity is along the negative direction of z-coordinate. After the establishment of the FEA model, the global stiffness matrix and global load vector can be exported for the optimal design of the fixture layout by the proposed method in Sec. 3.2.

3.2 Results of Optimal Design of Fixture Layout. Based on the FEA model in Sec. 3.1, we know that there are $m_1 = 2346$ and $m_2 = 392$ number of nodes on the curved part I and part II, respectively, thereby indicating $m = 2738$. $m_0 = 56$ number of nodes exist along the assembly interface between the curved panel I and panel II. $M_1 = M_2 = 6$ degrees-of-freedoms exist for each node of both panels, including three linear displacements and three angular displacements. Thus, there are $n_1 = 10{,}476$ and $n_2 = 2352$ number of nodal displacements for the curved part I and part II. The total number of fixtures $N = 30$ are used to support both curved compliant parts. The required precision of the surface profile tolerance is $\varepsilon = 3$. For the curved compliant part in the ship assembly process, the edge of the part cannot place fixtures, and the number of infeasible nodes of the curved part I and part

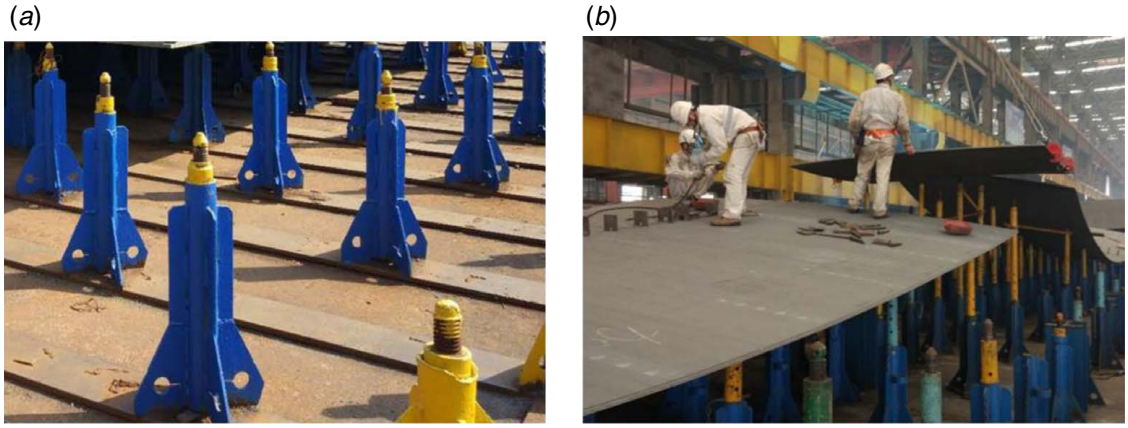

Fig. 3 The fixtures and fixture layout in a ship curved panel assembly process: (*a*) the fixtures used in the ship hull assembly, and (*b*) the assembly of curved panels

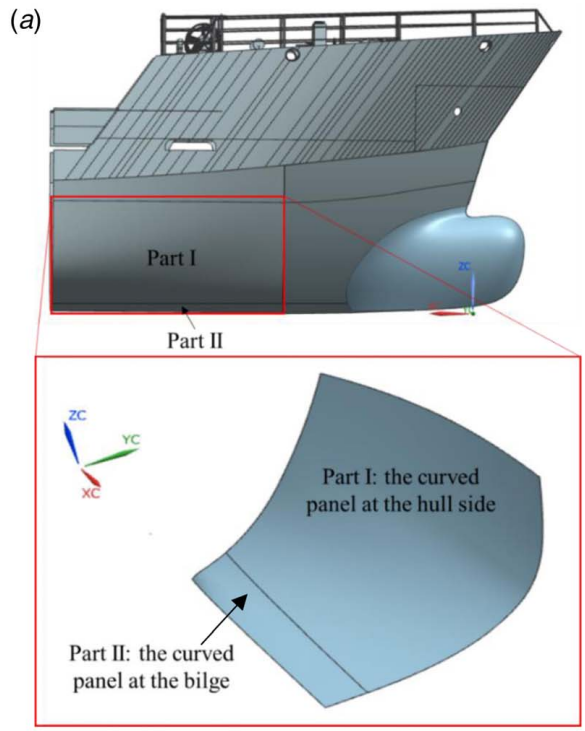

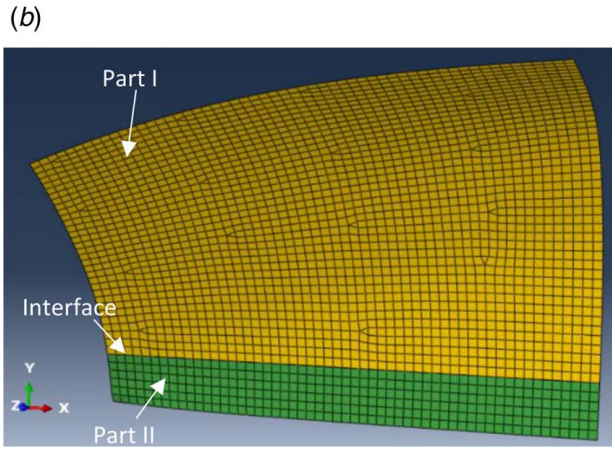

Fig. 4 (*a*) The geometry and (*b*) FEA model of the compliant curved panels to be assembled

II are $c_1 = 189$ and $c_2 = 122$. Thus, we use the formulation (8) to optimize the fixture layout for this case study.

According to the general practice of simulated annealing, the parameters in Algorithm 1 are set as $T = e^8$, $\beta^0 = 1.1$, $\alpha = 1.25$, $L = 30$, and $\delta = 1000$. The initial state of fixture layout $\boldsymbol{x}^0$ is randomly selected from the feasible set. In this case study, the "*N*-2-1" locating principle of Cai et al. [17] is adopted, and the positions of "2-1" locators on the secondary and tertiary datums are known in practice. "*N*" fixtures on the primary datum play a key role on reduction of the deformation caused by the gravity. Thus, we mainly focus on the optimization of "*N*" fixture layout. Generally, the number of $N = 30$ fixtures only constrain the linear displacements in *z*-direction, so only the linear displacements in *z*-direction are zero. The three locators will only constrain the linear displacement in either *x*-direction or *y*-direction according to the "*N*-2-1" locating principle. Given $\boldsymbol{x}^0$ and the positions of locators, the modified stiffness matrix $\bar{\mathbf{K}}_1(x^0)$ and modified nodal force vector $\bar{\mathbf{f}}(x^0)$ can be obtained from Proposition 1, and we optimize the fixture layout of the *N* fixtures. Figure 5 shows the feasible, infeasible, proposed fixture layout and three locators of the curved panels to be assembled on the *x*–*y* projection. As shown in Fig. 5, the proposed optimal design of the fixture layout tends to distribute more fixtures close to the longer edge, which is consistent with engineering intuition.

In current practice, a uniform fixture layout is adopted for the curved part assembly, as shown in Fig. 6. Our method optimizes the fixture layout for both parts together and places 25 fixtures for part I and five fixtures for part II. In this way, our method can

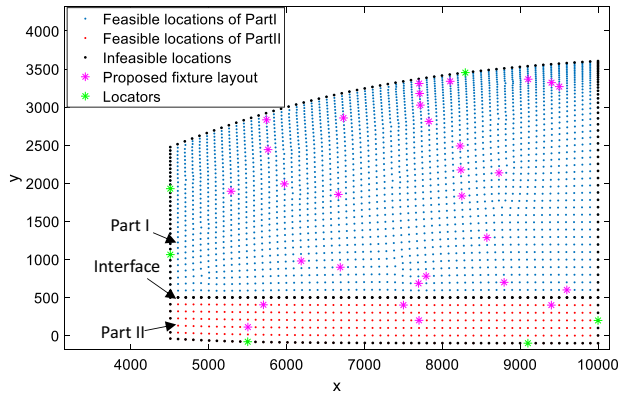

Fig. 5 Illustrations of feasible, infeasible locations, locators of part I and part II, and the proposed optimal design of the fixture layout

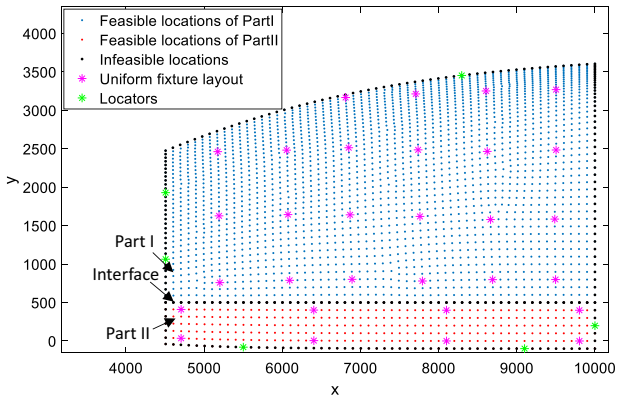

Fig. 6 Illustrations of feasible, infeasible locations, locators of part I and part II, and the current practice of the fixture layout

reduce the large deformation of part I as well as achieve good profile dimension of part II. To quantitatively compare the proposed method with the current practice, we introduce the mean and maximum of nodal dimensional gaps to evaluate both methods. As shown in Table 1, the optimal designed fixture achieves 89.17% less mean and 70.85% less maximum of the dimensional gaps. Table 1 also lists the maximum of displacements of the compliant parts to be assembled. Notably, our method significantly reduces the maximum displacement of the compliant part assembly and meets the required precision of surface profile precision. By comparison, the current practice needs more fixtures to satisfy this requirement. Thus, our method can achieve high precision part set up for assembly with a smaller number of fixtures comparing with the current practice.

To further illustrate the comparison results between our method and the current practice, we also show the nodal deformations of the curved parts to be assembled in Fig. 7. Figures 7(*a*)–7(*c*) show deformations in the *x*-, *y*-, and *z*-directions, and the color shows the deformation magnitude. The color difference along the assembly interface of two compliant parts indicates the gap magnitude. In another word, a larger color difference indicates a larger gap. We marked two lager gaps on Figs. 7(*b*) and 7(*c*). Compared with current practice, the deformation color of our method is more consistent along the assembly interface, thereby indicating smaller dimensional gap due to the optimal design of the fixture layout. As shown in Fig. 7(*b*), the deformation in the *y*-direction is more significant than other directions. This is because part II is almost set in the *x*–*y* plane, as shown in Fig. 8, so the deformation in the *y*-direction is very small. Part I is a curved panel with large radians and most of its area is in the *x*–*z* plane, so the deformation in the *y*-direction of part I is more significant.

Notably, no setup errors are considered in our method and current practice. Our paper focuses on the optimal design of the fixture layout on the part, and in the simulation, we precisely use the dimension of our optimization result to generate and evaluate the gaps. Thus, the dimensional gap is purely caused by the gravity deformations of part I and part II given different fixture layouts. Deformations of part I and part II in current practice are significantly different due to the non-optimal design of the fixture layout, thereby leading to large dimensional gaps.

Table 1 Linear displacement (mm) comparisons given the fixture layout from our method and current practice in the ship curved part assembly

Method	Mean gap	Max gap	Max displacement
Our method	0.17	0.58	2.92
Current practice	1.57	1.99	4.86
Reduction percentage	89.17%	70.85%	39.92%

In this paper, the dimensional gap along the assembly interface is the key concern for seam welding quality in the ship assembly process. Thus, the objective of optimal layout of fixture design is to minimize the dimensional gap along the interface between two assembly parts under the constraint of surface profile tolerance ε. Given such objective, the optimization algorithm will try the best to minimize the gap and panel deformation induced by gravity to meet the tolerance requirement. Figure 9 further shows dimensional gaps of the assembly interface between two parts by our method and current practice, and our method achieves significant gap reduction, which will significantly improve seam welding during assembly. Therefore, the proposed fixture layout shows superior performance than the current practice.

In order to better show the comparison results, the statistical evidence is also provided. The paired-sample *t*-test is used to test the mean difference between the proposed fixture layout and the current practice. The null hypothesis $H = 0$ is that no mean difference exists between the proposed fixture layout and the current practice. Otherwise, $H = 1$ indicates the null hypothesis is rejected at the 5% significance level. Table 2 lists the statistical test results including *H*-value, *p*-value, and 95% confidence interval (95% CI) of the mean difference. The statistical results show the significance of the proposed fixture layout over the current practice.

3.3 Finite Element Analysis Validation. In this subsection, we calculate the displacements of the parts and show the dimensional gaps of the assembly interface between these two curved panels under gravity by FEA via ABAQUS 6.13. The main objective of FEA validation is to further illustrate the dimensional gaps of the assembly interface and validate the accuracy of DSM for displacement calculations.

In order to clearly show the dimensional gaps along the assembly interface, we set the deformation scale factor as 100. The comparison results between our method and the current practice are shown in Fig. 10. Figure 10 illustrates the dimensional gaps along the interface in detail. When the proposed fixture layout is adopted, the max gap is on the left end of the assembly interface, and the gap gradually decreases first and then increases from the left end to the right end of the assembly interface (as shown in Fig. 10(*a*)). In contrast, when the current practice is adopted, the max gap is on the right end of assembly interface, and the gap gradually increases from the left end to the right end of the assembly interface (as shown in Fig. 10(*b*)). The dimensional gaps of current practice are much larger than our method. All of these results are consistent with the results shown in Fig. 9, which further validates the proposed method is effective to optimize the fixture layout in the ship curved panel assembly process.

In order to evaluate the accuracy of DSM, we calculated the displacement differences between DSM and FEA by the proposed fixture layout in this subsection. Table 3 lists the mean and maximum of the absolute differences and associated ratio of linear displacements calculated by DSM and FEA given the proposed fixture layout.

As shown in Table 3, the differences of displacement calculations by the DSM and FEA are very small, which are the numerical calculation difference. Thus, our method has a significant advantage that we do not need to do intensive FEA experiments from the commercial software or surrogate modeling from design of experiments but achieve accurate calculation of displacements during the optimal design of the fixture layout.

3.4 Discussion. In the literature, there are mainly two types of methods for the optimal design of the fixture layout for compliant parts, where the details are discussed in the introduction, i.e., Sec. 1. The first type of methods depend on the intensive FEA simulations from a commercial software, which is time-consuming and difficult to automate. To overcome such limitation, the second type of methods aim to establish surrogate models by using simulation data from FEA based on design of experiment. Machine

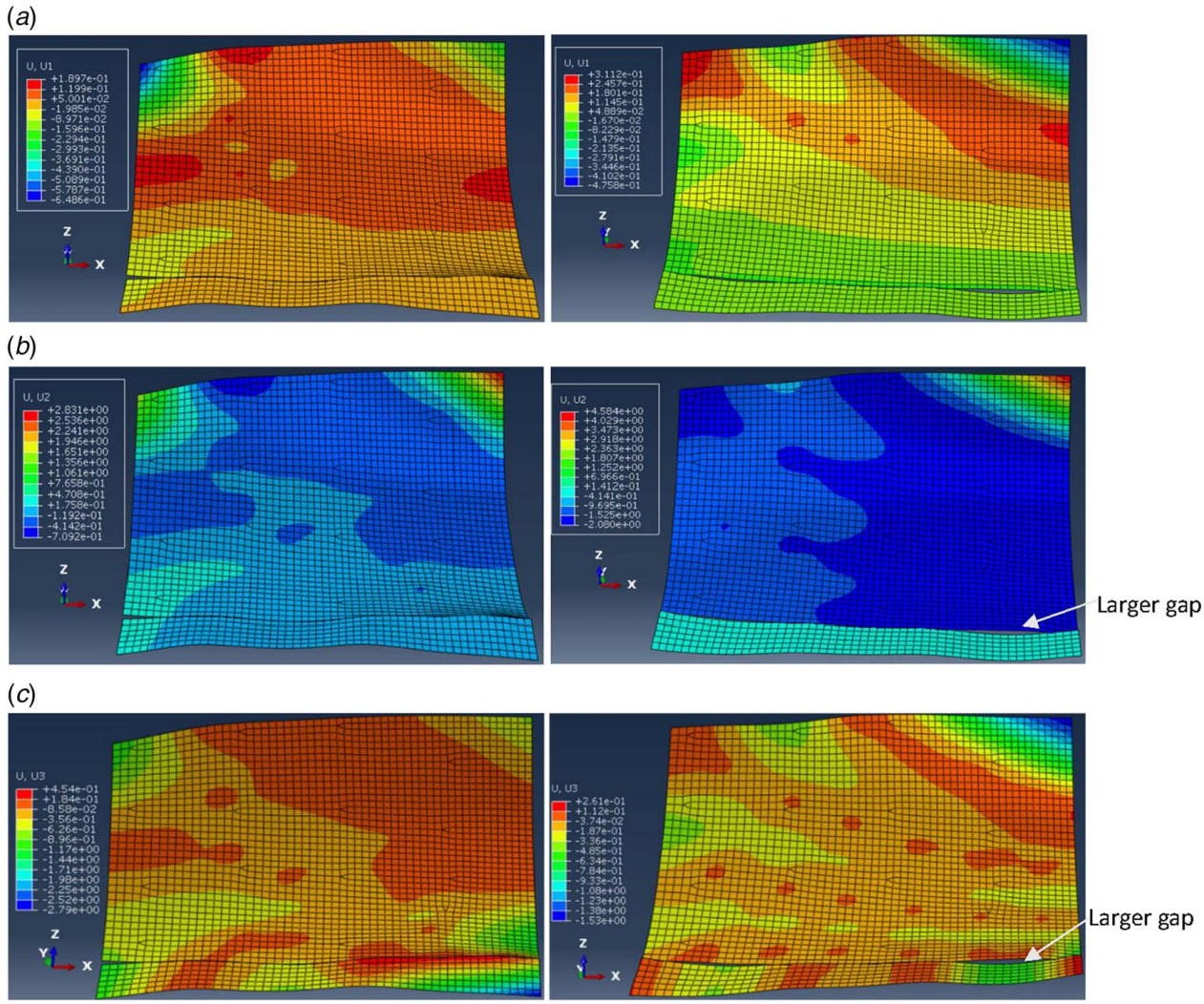

Fig. 7 Dimensional gaps of the assembly interface of our method (left) and current practice (right) in the (*a*) *x*-direction, (*b*) *y*-direction, and (*c*) *z*-direction: small gaps versus large gaps

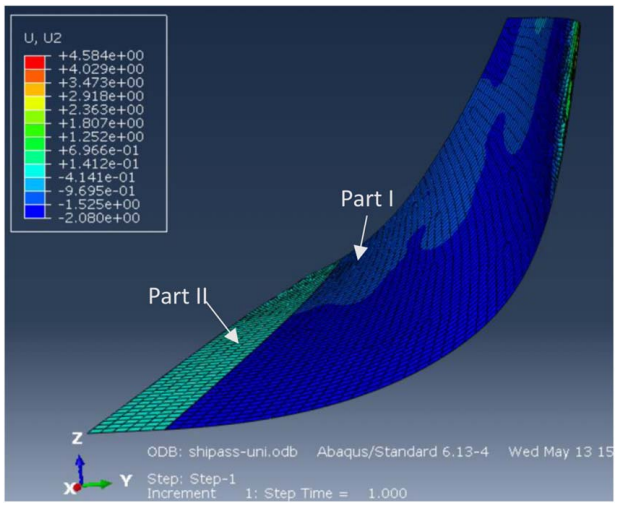

Fig. 8 Deformations in *y*-direction calculated by FEA

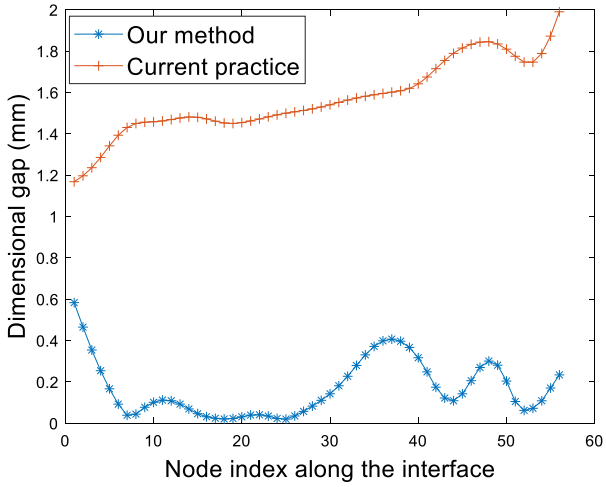

Fig. 9 Comparisons of dimensional gaps along the assembly interface between our method and current practice

Table 2 Statistical results of comparisons on the mean dimensional gap

H	p-value	95% CI
1	5.13×10^{-46}	[1.34, 1.46]

learning methods are applicable for surrogate modeling by collection of training dataset and testing dataset from FEA simulation. However, due to the following three reasons, the numerical comparisons between our method and those two types of methods are not necessary:

- In this paper, we proposed a physical model, i.e., modified direct stiffness method, to calculate the deformation under different fixture layouts instead of intensive FEA simulations. In addition, our method can reach the optimal fixture design automatically without calling FEA simulations during the optimization. In contrast, the first type of existing methods need intensive FEA simulations and call FEA software at each iteration step during optimization. Thus, although the computation load of FEA may be acceptable in practice, there are significant disadvantages of the FEA methods compared with our method.
- The surrogate modeling or data-driven models need a training dataset and a testing dataset, with both datasets generated from FEA simulations [30,31]. The procedures to do this will be (i) DOEs, (ii) FEA simulations to generate datasets based on DOE, and (iii) developments of data-driven models. The developed data-driven models can never be more accurate than the physical model from first principal. However, our physics-driven model (i.e., modified direct stiffness method) comes from first principal, which is the accurate model under the assumption of linear elastic deformation. Such assumption will be satisfied given suitable number of fixtures in the ship assembly process. Thus, the proposed physical model is more accurate and efficient than the surrogate model or data-driven models.
- The current literature [17,21] mainly aims to minimize the deflections of single part for fixture design, which cannot guarantee the dimensional gaps along the assembly interface. By comparison, we mainly focus on minimization of dimensional gaps to further improve the quality and efficiency of seam welding. Thus, if we numerically compare the dimensional gap between our method and existing methods, our methods will outperform other existing methods because we use the objective function of minimizing dimensional gaps along the interface between two compliant parts.

Currently, the initial value of N is determined by the engineering domain knowledge or experience. After the value of N is initialized, an iteritive trial-and-error procedure is followed via simulation studies to revise N to find the smallest N_0 that meets the tolerance "ε" of part deformations and gaps. If $N \geq N_0$, the precision requirement will be satisfied and will result in a smaller dimensional gap as N becomes larger.

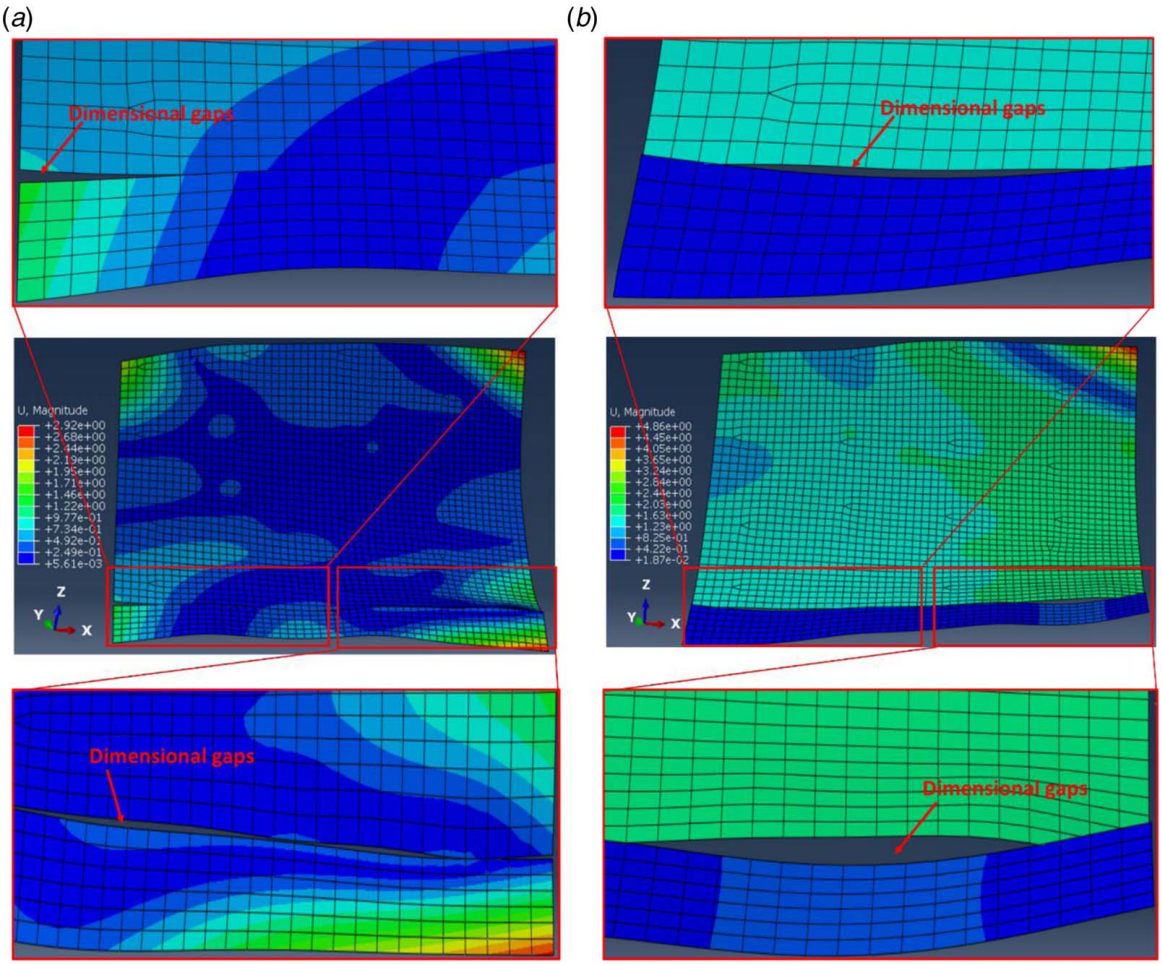

Fig. 10 Dimensional gaps along the assembly interface under different fixture layouts calculated by FEA: (*a*) our method and (*b*) current practice

Table 3 Displacement differences between DSM and FEA by the proposed fixture layout

Absolute difference	Part I	Part II
Maximum	4.94×10^{-6}	4.94×10^{-6}
Maximum ratio	4.67×10^{-6}	4.59×10^{-6}
Mean	3.36×10^{-7}	5.42×10^{-7}
Mean ratio	1.03×10^{-6}	9.01×10^{-7}

The largest dimension of the fixture layout optimization problem such as the number of fixtures N and the total number of nodes m are dependent on the computation power and delivery cycle of the assembly products. For example, in our case study, the computation time is 30,354.76 s, i.e., 8.43 h, on a laptop with Intel Core-i7-10710U @ 1.10 GHz processor, 16 GB of RAM, which meets the practice requirement since the fixture design is completed in the design stage.

The welding method used in the ship assembly process is arc welding or laser welding. During the welding process, two ship panels are welded by long continuous welding seam. The strength of welding seam is comparable with the material of assembled plates. Although there is grain coarsening at the high-temperature heat affected zone, it has no adverse effect on mechanical properties such as tensile, bend, and fatigue properties [41]. Thus, the subassembly can be regarded as one larger part with added dimensions of two assembled parts, and the proposed method is also applicable by using the stiffness matrix from the subassembly.

In practice, practitioners may need to do additional work to apply the proposed technique for fixture design compared with current practice. However, such analysis is only conducted once during the tooling design stage for the same type of assembly parts. Thus, it is still very beneficial for the industry to use this optimal design of the fixture layout to minimize the gap between two parts to be assembled, which leads to high welding quality, reduces the tooling adjustment, and reduces the cost.

This paper mainly focuses on the manufacturing design phase and aims to reduce the dimensional gaps along the assembly interface of compliant parts from the perspective of the optimal design of the fixture layout. In a compliant part assembly process, there are other factors that may result in dimensional varitions, such as part form errors, fixture errors, and setup errors. Considering such errors is important in practice for dimensional variation reduction and will be investigated in the future work.

4 Conclusion

This paper proposes a new method for the optimal design of fixture layouts. Due to the small ratio of the compliant part thickness to the length or the width and the large dimension, the deformation of compliant part induced by gravity is large, thereby leading to large dimensional gaps in the ship curved panel assembly process. However, dimensional gaps significantly influence the quality and efficiency of the seam welding during assembly. Thus, how to optimally determine the locations of fixtures to minimize dimensional gaps between two parts to be assembled is important but a challenging task. To tackle this challenge, we propose a binary integer programming formulation, which aims to minimize the dimensional gaps along the assembly interface between two parts to be assembled. In this way, we can improve the quality and efficiency of seam welding from the optimal design of the fixture layout. In addition, our method systematically integrates the direct stiffness method, which avoids the intensive FEA calculations from commercial software. A simulated annealing algorithm is further applied to obtain the optimal design of fixture layouts.

The case study shows that our method achieves satisfactory performance and outperforms current practice for the compliant parts in the ship curved panel assembly process in terms of the mean and maximum of dimensional gaps. The future study will be the dimensional variation analysis for the multi-stage ship curved panel assembly process.

Acknowledgment

The authors thank Mr. Shancong Mou from Georgia Tech for the kind discussions on the DSM. This research is sponsored by the Shanghai Sailing Program (Grant No. 20YF1420300), National Natural Science Foundation of China (Grant Nos. 52005371 and 72001139), and the Ministry of Industry and Information Technology of the People's Republic of China (Grant No. MC-201720-Z02).

Conflict of Interest

There are no conflicts of interest.

Data Availability Statement

The datasets generated and supporting the findings of this article are obtainable from the corresponding author upon reasonable request. The authors attest that all data for this study are included in the paper.

References

[1] McPherson, N. A., Galloway, A. M., and McGhie, W., 2013, "Thin Plate Buckling Mitigation and Reduction Challenges for Naval Ships," J. Mar. Eng. Technol., **12**(2), pp. 3–10.

[2] Huang, T. D., Dong, P., DeCan, L., Harwig, D., and Kumar, R., 2004, "Fabrication and Engineering Technology for Lightweight Ship Structures, Part 1: Distortions and Residual Stresses in Panel Fabrication," J. Ship Prod., **20**(1), pp. 43–59.

[3] Liu, C., Liu, T., Du, J., Zhang, Y., Lai, X., and Shi, J., 2020, "Hybrid Nonlinear Variation Modeling of Compliant Metal Plate Assemblies Considering Welding Shrinkage and Angular Distortion," ASME J. Manuf. Sci. Eng., **142**(4), p. 041003.

[4] Deng, D., Murakawa, H., and Ueda, Y., 2002, "Theoretical Prediction of Welding Distortion Considering Positioning and the Gap Between Parts," The Twelfth International Offshore and Polar Engineering Conference, Kitakyushu, Japan, May 26–31, pp. 337–343.

[5] Liang, W., and Deng, D., 2018, "Influences of Heat Input, Welding Sequence and External Restraint on Twisting Distortion in an Asymmetrical Curved Stiffened Panel," Adv. Eng. Softw., **115**, pp. 439–451.

[6] Penttilä, S., Kah, P., Ratava, J., and Pirinen, M., 2017, "Penetration and Quality Control With Artificial Neural Network Welding System," The 27th International Ocean and Polar Engineering Conference, San Francisco, CA, June 25–30, pp. 54–61.

[7] De Meter, E., 1995, "Min-Max Load Model for Optimizing Machining Fixture Performance," ASME J. Eng. Ind., **117**(2), pp. 186–193.

[8] Cai, W., Hu, S. J., and Yuan, J. X., 1997, "A Variational Method of Robust Fixture Configuration Design for 3-D Workpieces," ASME J. Manuf. Sci. Eng., **119**(4A), pp. 593–602.

[9] Kim, P., and Ding, Y., 2004, "Optimal Design of Fixture Layout in Multistation Assembly Processes," IEEE Trans. Autom. Sci. Eng., **1**(2), pp. 133–145.

[10] Kim, P., and Ding, Y., 2005, "Optimal Engineering System Design Guided by Data-Mining Methods," Technometrics, **47**(3), pp. 336–348.

[11] Phoomboplab, T., and Ceglarek, D., 2008, "Process Yield Improvement Through Optimum Design of Fixture Layouts in 3D Multistation Assembly Systems," ASME J. Manuf. Sci. Eng., **130**(6), p. 061005.

[12] Söderberg, R., and Carlson, J. S., 1999, "Locating Scheme Analysis for Robust Assembly and Fixture Design," Proceedings of the 1999 ASME Design Engineering Technical Conferences, Las Vegas, NV, Sept. 12–15.

[13] Lööf, J., Lindkvist, L., and Söderberg, R., 2009, "Optimizing Locator Position to Maximize Robustness in Critical Product Dimensions," ASME 2009 International Design Engineering Technical Conferences and Computers and Information in Engineering Conference, San Diego, CA, Aug. 30–Sept. 2, pp. 515–522.

[14] Söderberg, R., Lindkvist, L., and Carlson, J. S., "Managing Physical Dependencies Through Location System Design," J. Eng. Des., **17**(4), pp. 325–346.

[15] Rearick, M. R., Hu, S., and Wu, S., 1993, "Optimial Fixture Design for Deformable Sheet Metal Workpieces," Trans. NAMRI/SME, **11**, p. 407.

[16] Cai, W., and Hu, S., 1996, "Optimal Fixture Configuration Design for Sheet Metal Assembly With Springback," Trans. NAMRI/SME, **XXIV**, pp. 229–234.

[17] Cai, W., Hu, S. J., and Yuan, J. X., 1996, "Deformable Sheet Metal Fixturing: Principles, Algorithms, and Simulations," ASME J. Manuf. Sci. Eng., **118**(3), pp. 318–324.
[18] Das, A., Franciosa, P., and Ceglarek, D., 2015, "Fixture Design Optimisation Considering Production Batch of Compliant Non-Ideal Sheet Metal Parts," Procedia Manuf., **1**, pp. 157–168.
[19] Franciosa, P., Gerbino, S., and Ceglarek, D., 2016, "Fixture Capability Optimisation for Early-Stage Design of Assembly System With Compliant Parts Using Nested Polynomial Chaos Expansion," Procedia CIRP, **41**, pp. 87–92.
[20] Kulankara, K., Satyanarayana, S., and Melkote, S. N., 2002, "Iterative Fixture Layout and Clamping Force Optimization Using the Genetic Algorithm," ASME J. Manuf. Sci. Eng., **124**(1), pp. 119–125.
[21] Menassa, R., and DeVries, W., 1991, "Optimization Methods Applied to Selecting Support Positions in Fixture Design," ASME J. Eng. Ind., **113**(11), pp. 412–418.
[22] Dahlström, S., and Camelio, J. A., 2003 "Fixture Design Methodology for Sheet Metal Assembly Using Computer Simulations," ASME 2003 International Mechanical Engineering Congress and Exposition, Washington, DC, Nov. 15–21, pp. 321–328.
[23] Camelio, J. A., Hu, S. J., and Ceglarek, D., 2004, "Impact of Fixture Design on Sheet Metal Assembly Variation," J. Manuf. Syst., **23**(3), pp. 182–193.
[24] Liao, Y.-J., Hu, S., and Stephenson, D., 1998, "Fixture Layout Optimization Considering Workpiece-Fixture Contact Interaction: Simulation Results," Transactions of NAMRI/SME, **26**, pp. 341–346.
[25] Dou, J., Wang, X., and Wang, L., 2011, "Machining Fixture Layout Optimization Using Particle Swarm Optimization Algorithm," Fourth International Seminar on Modern Cutting and Measurement Engineering, Beijing, China, Dec. 10–12, vol. 7997, International Society for Optics and Photonics, p. 79970S.
[26] Cai, W., 2008, "Fixture Optimization for Sheet Panel Assembly Considering Welding Gun Variations," Proc. Inst. Mech. Eng. Part C: J. Mech. Eng. Sci., **222**(2), pp. 235–246.
[27] Xing, Y., Hu, M., Zeng, H., and Wang, Y., 2015, "Fixture Layout Optimisation Based on a Non-Domination Sorting Social Radiation Algorithm for Auto-Body Parts," Int. J. Prod. Res., **53**(11), pp. 3475–3490.
[28] Xing, Y., Chen, W., Li, X., Lu, J., and Zhang, H., 2015, "Multi-Station Fixture Location Layout Optimization Design for Sheet Metal Parts," J. Comput. Theor. Nanosci., **12**(9), pp. 2903–2908.
[29] Xing, Y., 2017, "Fixture Layout Design of Sheet Metal Parts Based on Global Optimization Algorithms," ASME J. Manuf. Sci. Eng., **139**(10), p. 101004.
[30] Yang, B., Wang, Z., Yang, Y., Kang, Y., and Li, X., 2017, "Optimum Fixture Locating Layout for Sheet Metal Part by Integrating Kriging With Cuckoo Search Algorithm," Int. J. Adv. Manuf. Technol., **91**(1–4), pp. 327–340.
[31] Lu, C., and Zhao, H.-W., 2015, "Fixture Layout Optimization for Deformable Sheet Metal Workpiece," Int. J. Adv. Manuf. Technol., **78**(1–4), pp. 85–98.
[32] Reddy, J., 2004, *An Introduction to the Finite Element Method*, McGraw-Hill, New York.
[33] Wu, B., Xu, Z., and Li, Z., 2008, "A Note on Imposing Displacement Boundary Conditions in Finite Element Analysis," Commun. Numer. Methods Eng., **24**(9), pp. 777–784.
[34] Korte, B., and Vygen, J., 2012, *Combinatorial Optimization*, Springer, Heidelberg.
[35] Blum, C., and Roli, A., 2003, "Metaheuristics in Combinatorial Optimization: Overview and Conceptual Comparison," ACM Comput. Surv. (CSUR), **35**(3), pp. 268–308.
[36] Weinan, E., Li, T., and Vanden-Eijnden, E., 2019, *Applied Stochastic Analysis*, American Mathematical Society, Providence.
[37] Smith, A. E., and Coit, D. W., 1997, "Penalty Functions," Handb. Evol. Comput., **97**(1), p. C5.
[38] Beichl, I., and Sullivan, F., 2000, "The Metropolis Algorithm," Comput. Sci. Eng., **2**(1), pp. 65–69.
[39] Talatahari, S., Alavi, A. H., and Gandomi, A. H., 2013, *Metaheuristics in Water, Geotechnical and Transport Engineering*, Elsevier Science and Technology Books, Incorporated, Newnes.
[40] Stewart, M. L., 2004, "Variation Simulation of Fixtured Assembly Processes for Compliant Structures Using Piecewise-Linear Analysis," Dissertation, Brigham Young University.
[41] Taban, E., Deleu, E., Dhooge, A., and Kaluc, E., 2009, "Laser Welding of Modified 12% Cr Stainless Steel: Strength, Fatigue, Toughness, Microstructure and Corrosion Properties," Mater. Des., **30**(4), pp. 1193–1200.